HAL open science

Dynamic Behavior of Very-High Speed Rotors at Non-stationary Conditions

Emna Sghaier, Adeline Bourdon, Didier Remond, Jean-Luc Dion, Nicolas Peyret

To cite this version:

Emna Sghaier, Adeline Bourdon, Didier Remond, Jean-Luc Dion, Nicolas Peyret. Dynamic Behavior of Very-High Speed Rotors at Non-stationary Conditions. Proceedings of the 10th International Conference on Rotor Dynamics – IFToMM Vol 4, 63, Springer International Publishing, pp.79-90, 2019, Mechanisms and Machine Science, 10.1007/978-3-319-99272-3_6 . hal-03991334

HAL Id: hal-03991334

https://hal.science/hal-03991334

Submitted on 6 Jun 2023

HAL is a multi-disciplinary open access archive for the deposit and dissemination of scientific research documents, whether they are published or not. The documents may come from teaching and research institutions in France or abroad, or from public or private research centers.

L'archive ouverte pluridisciplinaire **HAL**, est destinée au dépôt et à la diffusion de documents scientifiques de niveau recherche, publiés ou non, émanant des établissements d'enseignement et de recherche français ou étrangers, des laboratoires publics ou privés.

Distributed under a Creative Commons Attribution - NonCommercial 4.0 International License

Dynamic Behavior of Very-High Speed Rotors at Non-stationary Conditions

Emna Sghaier[1,2(✉)], Adeline Bourdon[1], Didier Remond[1], Jean-Luc Dion[2], and Nicolas Peyret[2]

[1] LaMCoS, INSA-Lyon, CNRS UMR5259, University of Lyon, 69621 Lyon, France
emna.sghaier@insa-lyon.fr
[2] Laboratoire QUARTZ EA 7393 - SUPMECA Paris, 3 rue Fernand Hainaut, 93400 Saint Ouen, France

Abstract. Speed reducers with input shafts spinning at very high speeds (up to 42 000 rpm) are generally associated to electric motors, which are more and more used especially in the automotive field, in order to bring the rotational speed to the most efficient window. Accurate modeling of those rotating machinary behavior is crucial to improve product reliability and to prolong machinery life. Many studies are conducted with an imposed angular speed, which is in most of the cases considered as constant or, in best cases, which follows a given variation law. In this paper, the study is performed with no assumption on the rotational speed. A variable driving torque is induced to the input shaft and the instantaneous angular speed (IAS) is deduced from the dynamic problem coupled to an angular approach. As a result, the IAS takes into account not only the induced torque perturbations but also the periodic geometry of the whole structure (e.g.: bearings and gears). The aim of this work is to extend the existing model based on the Finite Element Method by introducing an enhancement of the gyroscopic effect matrices without any assumption on the spinning speed. This model will lead to the introduction of coupling between the flexural and torsional degrees of freedom as well as to a non-linearity in the modeling of the studied system. The aim is to improve the accuracy of simulations for the rotor dynamics in non-stationary conditions especially when getting through critical speeds.

Keywords: Rotor dynamics · Gyroscopic effect
Non-stationary conditions · Very-high speed
Instantanious angualr speed (IAS)

1 Introduction

The dynamic behavior of rotating machinery is often made on the assumption of constant speed. The angular speed follows then a given law of variation during the time. Some were interested in studying the rotor's behavior in transient motion during start up and shutdown operations [1]. They impose a perfect linear or exponential law of variation for the speed of rotation. It was demonstrated

that the amplitude of the unbalance response of a rotor which runs through critical speed can be reduced by increasing the rate of acceleration. Genta and Delprete [2] were interested in the case of torsionnally stiff rotor running with a given law. They extended the formulation of a multi-degree-of-freedom rotors operating at variable speeds to include the effects of non-linearities and the lack of axial symmetry. Al-Bedoor [3], in his works, studied the coupled torsional and lateral vibrations of unbalanced Jeffcot rotors. He considered the rotor rigid-body rotation and the torsional deformation angle as two seperate degrees of freedom. Gyroscopic effects due to disk spinning were neglected and his mathematical model was limited to speed of rotations below the second lateral critical speed. Roques et al. [4] studied the case of transient response induced by rotor-to-stator rubbing caused by a sudden blade-off. They considered that the angular position is an unknown of the dynamic problem in order to assess the angular deceleration and characterize the transient reponse of the shaft during rubbing. However, they assume that the torsional vibrations are negligible and they are not considered in the governing equations of motion of the rotor. Li et al. [5] developed an analytical closed-form solutions for the transient envelopes corresponding to the amplification of the solution of displacement, velocity and acceleration through the critical speed during run-up or run down process. Yamamoto [6] considered a rotor with a periodically fluctuating rotational speed. He assumed that there is no coupling between torsional and lateral vibrations and examined the forced response to an external effort. Under those assumptions his dynamic model resulted on equations of motion with time varying coeffiecients. He showed that, contrary to expectations, this time varying coefficients do not necessarily lead to unstable behavior of the rotor.

In this study, we suggest not to make any assumption on the angular speed. The rotor shaft is flexible in traction, bending and torsion. A driving torque is induced to the shaft and the angular displacement including both the rigid body motion and the torsional deformation is assessed. Nevertheless, we keep the assumption of small displacements and 'rotations' and small unbalance. The model accounts for the effects of rotating inertia, shear deformation and gyroscopic effect. A main emphasis is put on the new formulation of the gyroscopic effect under non-stationary working conditions.

2 Dynamic Behavior of the Rotor

The basic elements of the rotor are the disk, the shaft and the bearings. A mass unbalance, which is unavoidable in the manufacturing process, is also considered. The calculation of the kinetic and strain energy leads to the governing equations of the dynamic behavior of the rotor by the application of Lagrange equations. The bending and torsional vibrational behavior of the rotor, passing its critical speeds under a driving torque is considered.

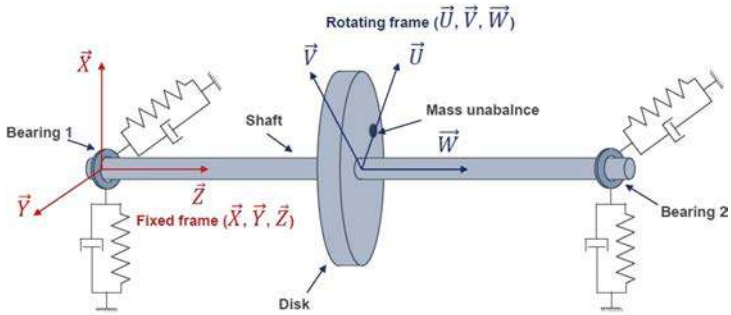

Fig. 1. Studied system

2.1 System Description

The coordinate systems used in developing the model are shown in the following figure, wherein, (XYZ) is the fixed reference frame and (UVW) is the rotating reference frame which coincides with the principle axis of the cross section of the shaft. To describe the general orientation of the cross-section of the shaft element one first rotates by an angle Φ about the $Z-$axis then by an angle θ about the new X'-axis and finally by an angle Ψ about the final W'-axis. This choice of Euler angles was used by Hsieh et al. [7] to describe the orientation of the rotating element (Fig. 1).

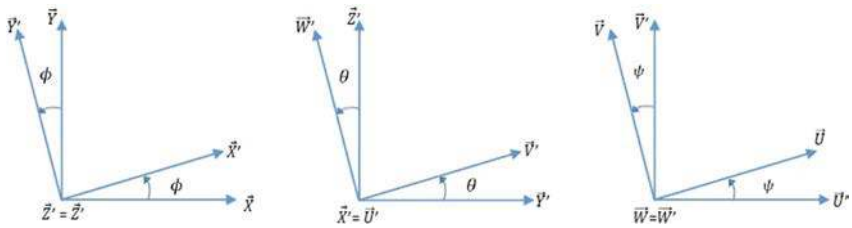

Fig. 2. The rotor coordinate systems

The angular displacement about the X and Y axis are calculated using Euler angles as follows (Fig. 2):

$$\theta_x = \theta.cos(\phi) \tag{1a}$$

$$\theta_y = \theta.sin(\phi) \tag{1b}$$

The spinning angle about the axis Z is given by:

$$\theta_z = \phi + \psi \tag{2}$$

It is very important to notice here that θ_z accounts for both the free body rotating motion as well as for the torsional deformation.

The instantaneous angular velocity vector, projected on the rotating frame (UVW), may be expressed as:

$$\omega_u = \dot{\theta}cos(\psi) + \dot{\phi}sin(\theta)sin(\psi) \tag{3a}$$

$$\omega_v = -\dot{\theta}sin(\psi) + \dot{\phi}sin(\theta)cos(\psi) \tag{3b}$$

$$\omega_w = \dot{\psi} + \dot{\phi}cos(\theta) \tag{3c}$$

Using this angular velocity description in the frame described by the directions of the principle axis, the kinetic energy part related to the rotating motion is calculated.

2.2 Disk Equations

We assume that the disk is rigid. It is then fully characterized by its kinetic energy associated to the displacement of its center of mass C (u_c, v_c, w_c) and to the rotational motion of its section. It is found to be:

$$T_D = \frac{1}{2}[m_D(\dot{u_c}^2+\dot{v_c}^2+\dot{w_c}^2)+I_{Dw}\dot{\theta}_{z_c}^2+I_{Dw}\dot{\theta}_{z_c}(\dot{\theta}_{x_c}\theta_{y_c}-\dot{\theta}_{y_c}\theta_{x_c})+I_{Du}(\dot{\theta_{x_c}}^2+\dot{\theta_{y_c}}^2)] \tag{4}$$

Equation (4) exhibits explicitly the anti-symmetry of the rotor's flexural behavior in both of (xoz) and (yoz) planes.

The displacement vector of the mass center C, denoted $\{\delta_c\}$, is modeled with six degrees of freedom, three translations and three rotations, as follows:

$$\{\delta_c\}^t = \{u_c, v_c, w_c, \theta_{x_c}, \theta_{y_c}, \theta_{z_c}\}_{\{1,6\}} \tag{5}$$

The application of Lagrange equation leads to the following matrix equation:

$$\frac{d}{dt}\left(\frac{\partial T_D}{\partial \dot{\delta}}\right) - \frac{\partial T_D}{\partial \delta} = [M_D(\{\delta_c\})]\left\{\ddot{\delta}\right\} + \left[C_D(\dot{\theta}_{z_c})\right]\left\{\dot{\delta}\right\} \tag{6}$$

such as:

$$[M_D(\{\delta_c\})]_{(6,6)} = \begin{bmatrix} m_D & 0 & 0 & 0 & 0 & 0 \\ 0 & m_D & 0 & 0 & 0 & 0 \\ 0 & 0 & m_D & 0 & 0 & 0 \\ 0 & 0 & 0 & I_{Du} & 0 & \frac{I_{Dw}}{2}\theta_{y_c} \\ 0 & 0 & 0 & 0 & I_{Du} & -\frac{I_{Dw}}{2}\theta_{x_c} \\ 0 & 0 & 0 & \frac{I_{Dw}}{2}\theta_{y_c} & -\frac{I_{Dw}}{2}\theta_{x_c} & I_{Dw} \end{bmatrix}$$

and $\left[C_D(\dot{\theta}_{z_c})\right]$ is the classical skew-matrix related to the gyroscopic effects.

The matrix $[M_D]$ is no longer a diagonal matrix as it is the case when studying the stationary regime, it has extra-diagonal terms variable with time due to the assumption of non-stationary regime inducing coupling between flexural and torsional behavior. This matrix is dissociated to a constant diagonal matrix and a time varying matrix with only time-varying extra-diagonal terms as follows:

$$[M_D(\{\delta_c\})]_{\{6,6\}} = [M_{Dconst}]_{\{6,6\}} + [M_{Dvar}(\{\delta_c\})]_{\{6,6\}} \tag{7}$$

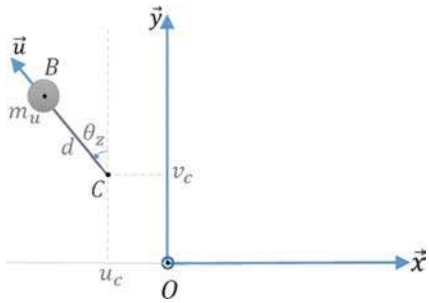

Fig. 3. Illustration for the mass unbalance

2.3 Mass Unbalance

The mass unbalance is defined by its mass m_u situated at a distance d from the geometric center of the shaft $C(u_c, v_c)$. The calculation of the kinetic energy related to the presence of a mass unbalance T_u and the application of Lagrange equations lead to the following matrix form (Fig. 3):

$$\frac{d}{dt}\left(\frac{\partial T_u}{\partial \dot{\delta}}\right) - \frac{\partial T_u}{\partial \delta} = [M_u(\theta_{z_c})]\left\{\ddot{\delta}\right\} + \{F_{nl_u}(\theta_{z_c})\} \tag{8}$$

where

$$[M_u(\theta_{z_c})] = d\, m_u \begin{bmatrix} 0 & 0 & 0\,0\,0 & cos(\theta_{z_c}) \\ 0 & 0 & 0\,0\,0 & -sin(\theta_{z_c}) \\ 0 & 0 & 0\,0\,0 & 0 \\ 0 & 0 & 0\,0\,0 & 0 \\ 0 & 0 & 0\,0\,0 & 0 \\ cos(\theta_{z_c}) & -sin(\theta_{z_c}) & 0\,0\,0 & d \end{bmatrix}_{\{6,6\}}$$

$$\{F_{NL_u}(\theta_{z_c})\} = -d\, m_u\, \dot{\theta}_{z_c}^2 \begin{Bmatrix} sin(\theta_{z_c}) \\ cos(\theta_{z_c}) \\ 0 \\ 0 \\ 0 \\ 0 \end{Bmatrix}_{\{6,1\}}$$

In addition to the classical centrifugal force, due to the non-stationary regime working condition, an additional mass matrix with time varying components is also obtained. Again, this matrix reflects a coupling between the flexural behavior and the torsional one.

2.4 The Shaft Element Equations

The element shaft is flexible in traction-compression, bending and torsion. It has a cylindrical cross-section. The equation of the dynamic behavior are obtained, as previously, by writing the Lagrange equations.

We first calculate the kinetic energy, which, over a shaft element, is obtained by integrating over the length element l as follows:

$$T_s = \frac{\rho S}{2}\int_0^l (\dot{u_c}^2 + \dot{v_c}^2 + \dot{w_c}^2)\,\mathrm{d}z + \rho I_p \int_0^l \dot{\theta}_z^2\,\mathrm{d}z + \rho I_p \int_0^l \dot{\theta}_z(\dot{\theta}_x\theta_y - \dot{\theta}_y\theta_x)\,\mathrm{d}z + \frac{\rho I_d}{2}\int_0^l (\dot{\theta_x}^2 + \dot{\theta_y}^2)\,\mathrm{d}z \tag{9}$$

In order to describe, using the finite element method, the flexural motion of the shaft in both of the lateral directions, we define, for each elemet shaft both vectors $\{\delta u\}^t = \langle u_1, \theta_{y1},\, u_2, \theta_{y2}\rangle$ and $\{\delta v\}^t = \langle v_1, \theta_{x1},\, v_2, \theta_{x2}\rangle$ as shown in Figs. 4 and 5. Whereas the axial and torsional displacements are descritized using respectively both vectors $\{\delta w\}^t = \langle w_1,\, w_2\rangle$ and $\{\delta\theta_z\}^t = \langle \theta_{z1}, \theta_{z2}\rangle$.

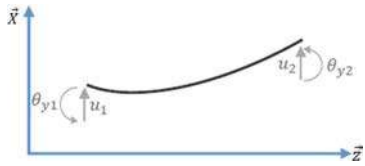

Fig. 4. Flexural degrees of freedom on the XZ plane of a beam element

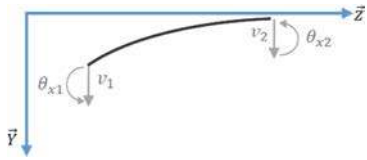

Fig. 5. Flexural degrees of freedom on the YZ plane of a beam element

We also define the nodal displacement vector accounting at once for translation, flexion and torsion as:

$$\{\delta_e\}^t = \{u_1,\ v_1,\ w_1,\ \theta_{x1},\ \theta_{y1},\ \theta_{z1},\ u_2,\ v_2,\ w_2,\ \theta_{x2},\ \theta_{y2},\ \theta_{z2}\}^t_{(1,12)} \tag{10}$$

Using the finite element method, we obtain the following expression for the kinetic energy over a shaft element:

$$T_{s_e} = \frac{1}{2}\{\dot{\delta_e}\}^t[M_{s_e}]\{\dot{\delta_e}\} + T_{gyr_e} \tag{11}$$

where $[M_{s_e}]$ is the elementary mass matrix including both the classical mass matrix and the secondary effects of the rotatory inertia matrix. T_{gyr_e} is the gyroscopic effect expression such as:

$$\begin{aligned} T_{gyr_e} = & -\rho I_p \int_0^l \langle N_3 \rangle \left\{ \delta \dot{\theta}_z \right\} \left\langle \frac{\partial N_2}{\partial z} \right\rangle \{\delta \dot{v}\} \left\langle \frac{\partial N_1}{\partial z} \right\rangle \{\delta u\} \, \mathrm{d}z \\ & + \rho I_p \int_0^l \langle N_3 \rangle \left\{ \delta \dot{\theta}_z \right\} \left\langle \frac{\partial N_1}{\partial z} \right\rangle \{\delta \dot{u}\} \left\langle \frac{\partial N_2}{\partial z} \right\rangle \{\delta v\} \, \mathrm{d}z \end{aligned} \tag{12}$$

$\langle N_1 \rangle$, $\langle N_2 \rangle$ are vectors with cubic shape functions and $\langle N_3 \rangle$ is a vector with linear ones.

In order to be able to write the kinetic energy related to the gyroscopic effect under a matrix form, we proceed by an integration by parts, which leads to the following formulation for the gyroscopic effects:

$$\frac{d}{dt} \left(\frac{\partial T_{gyr_e}}{\partial \dot{\delta}_e} \right) - \frac{\partial T_{gyr_e}}{\partial \delta_e} = [S_{gyr_e}(\{\delta_e\})] \{\ddot{\delta}_e\} + \{Fnl_{gyr_e}(\{\dot{\delta}_e\})\} \tag{13}$$

where:

$$\begin{aligned} \left[S_{gyr_e}(\{\delta_e\}) \right] = & -\langle N_3(l) \rangle^t \{\delta_e\}^t [M_{67}^g(l)]^t - [M_{67}^g(l)] \{\delta_e\} \langle N_3(l) \rangle \\ & + \left\langle \frac{\partial N_3}{\partial z} \right\rangle^t \{\delta_e\}^t [M_{67}^{g*}(l)]^t + [M_{67}^{g*}(l)] \{\delta_e\} \left\langle \frac{\partial N_3}{\partial z} \right\rangle \end{aligned} \tag{14}$$

$$\begin{aligned} \{Fnl_{gyr_e}(\{\dot{\delta}_e\}, \{\dot{\delta}_e\})\} = & -\langle N_3(l) \rangle^t \left(\{\dot{\delta}_e\}^t [M_{67}^g(l)] \{\dot{\delta}_e\} \right) \\ & - 2 \left(\langle N_3(l) \rangle \{\dot{\delta}_e\} \right) \left([M_{67}^g(l)] \{\dot{\delta}_e\} \right) \\ & + \left\langle \frac{\partial N_3}{\partial z} \right\rangle^t \left(\{\dot{\delta}_e\}^t [M_{67}^{g*}(l)] \{\dot{\delta}_e\} \right) \\ & + 2 \left(\left\langle \frac{\partial N_3}{\partial z} \right\rangle \{\dot{\delta}_e\} \right) \left([M_{67}^{g*}(l)] \{\dot{\delta}_e\} \right) \end{aligned} \tag{15}$$

such as

$$[M_{67}^g(l)]_e = \rho I_p \int_0^l \left(\left\langle \frac{\partial N_2}{\partial z} \right\rangle^t \left\langle \frac{\partial N_1}{\partial z} \right\rangle - \left\langle \frac{\partial N_1}{\partial z} \right\rangle^t \left\langle \frac{\partial N_2}{\partial z} \right\rangle \right) \mathrm{d}z \tag{16a}$$

$$[M_{67}^{g*}(l)]_e = \rho I_p \int_0^l \left(\int_0^z \left(\left\langle \frac{\partial N_2}{\partial z} \right\rangle^t \left\langle \frac{\partial N_1}{\partial z} \right\rangle - \left\langle \frac{\partial N_1}{\partial z} \right\rangle^t \left\langle \frac{\partial N_2}{\partial z} \right\rangle \right) \mathrm{d}z \right) \mathrm{d}z \tag{16b}$$

The application of the Lagrange equations on the kinetic energy of the shaft element leads to:

$$\frac{d}{dt} \left(\frac{\partial T_{s_e}}{\partial \dot{\delta}_e} \right) - \frac{\partial T_{s_e}}{\partial \delta_e} = [M_{s_e}] \{\ddot{\delta}_e\} + [S_{gyr_e}(\{\delta_e\})] \{\ddot{\delta}_e\} + \{Fnl_{gyr_e}(\{\dot{\delta}_e\})\} \tag{17}$$

$[S_{gyr_e}(\{\delta_e\})]$ and $\{Fnl_{gyr_e}(\{\dot{\delta_e}\})$ induce a strong non linearity to the system and coupling between the lateral and torsional degrees of freedom.

The calculation of the strain energy of the shaft and the virtual works of the bearings, assumed to be with linear stiffness and damping, leads to the classical stiffness matrix and we finally write the equation of the dynamics of rotating shaft element such as:

$$[M_{s_e}]\{\ddot{\delta_e}\}+[C_{s_e}]\{\dot{\delta_e}\}+[K_{c_e}]\{\delta_e\}=-[S_{gyr_e}(\{\delta_e\})]\{\ddot{\delta_e}\}-\{Fnl_{gyr_e}(\{\dot{\delta_e}\})\} \quad (18)$$

2.5 Equations of the Rotor

Once the contribution of each of the constitutive elements of the rotor calculated, we consider them thoroughly to write the equation of the dynamic behavior of the rotor. As we have seen previously, the vector and matrix related to the gyroscopic effect depends explicitly on the displacement and velocity vectors $\{\delta_e\}$ and $\{\dot{\delta_e}\}$. We need then, to evaluate those vectors at each time step before doing the assembly over all the shaft elements. The choice of an explicit integration scheme is made. At each time step t_{i+1}, vectors $\{\delta\}_{t_i}$ and $\{\dot{\delta}\}_{t_i}$ are assumed to be known and then the gyroscopic effect terms over an element, namely $[S_{gyr_e}(\{\delta_e\})]$ and $\{Fnl_{gyr_e}(\{\dot{\delta_e}\})\}$ are calculated and assembled over the whole shaft.

Finally, the equation of motion, in the presence of external efforts can be written as follows:

$$\begin{aligned}
&([M_s]+[M_{D_{const}}])\{\ddot{\delta}\}_{i+1}+[C_s]\{\dot{\delta}\}_i+[K_c]\{\delta\}_i= \\
&\quad -([S_{gyr}(\{\delta\}_i)]+[M_{D_{var}}(\{\delta\}_i)]+[M_u(\theta_{z_c})]_i)\{\ddot{\delta}\}_{i+1} \\
&\quad -\left[C_D(\dot{\theta}_{z_c})\right]_i\{\dot{\delta}\}_i \\
&\quad -\left(\{Fnl_{gyr}(\{\dot{\delta}\}_i)\}+\{F_{nl_u}(\theta_{z_c})\}_i\right) \\
&\quad +\{F_{ext}\}_i
\end{aligned} \quad (19)$$

where in the left side of the equation, the terms which are constant at each time step and, in the right side, the ones which need to be updated at every time step.

3 Exemple of a Rotor at Non-stationary Working Conditions

We consider a rotor made of a shaft and a disk with a mass unbalance (Fig. 6) with the properties summerized in Table 1. The shaft is descritized into 10 finite elements and the disk is situated at the node number 7 (from the left) as well as the mss unbalance.

We calculate the response of the rotor to a mass unbalance when it is driven by a torque which is constant in the beginning and then, after $1\,s$, follows a linear low as a function of time (Fig. 7).

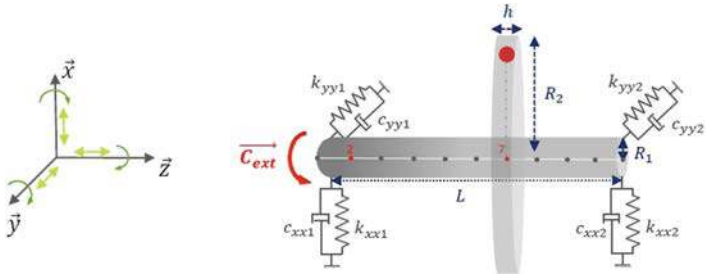

Fig. 6. Rotor model

Table 1. Proprieties of the rotor

Symbol	Quantity	Value
L	Shaft length	0.6 m
R_1	Shaft radius	0.01 m
R_2	Disk radius	0.08 m
h	Thickness of the disk	0.03 m
ρ	Mass per unit volume	7800 $kg.m^{-3}$
E	Young modulus	2.10^{11} $N.m^{-2}$
m_u	Mass unbalance	1% of the mass of the disk
d	Eccentricity of the mass unbalance	0.1m
k_{xx1}, k_{xx2}	Stiffness along x-axis of the left and right bearings	$1.e^8$ $N.m^{-1}$
k_{yy1}, k_{yy2}	Stiffness along y-axis of the left and right bearings	$1.e^8$ $N.m^{-1}$
c_{xx1}, c_{xx2}	Damping along x-axis of the left and right bearings	$2e2$ $N.s.m^{-1}$
c_{yy1}, c_{yy2}	Damping along y-axis of the left and right bearings	$2e2$ $N.s.m^{-1}$

As it is highlighted by Srinivasan et al. [8], it is very important to provide a sufficient torque so that the rotating machinary doesn't stall below the target speed. They explained that, when the speed of rotation coincides with a lateral critical speed the amplitude of the vibrations may increase to levels high enough to trip the machine. They called this phenomenon limited torque-acceleration of rotors through the critical speed.

When spinning at very high speeds, rotors may encounter more than one critical speed. If the rotor passes easily through the first one, it can have more difficulties going through the second one as showed in Fig. 8: The instantanious angular velocity is slightly disturbed when crossing the first critical speed at 2 527 rpm. But when crossing the second critical speed at 26 364 rpm, the rotor

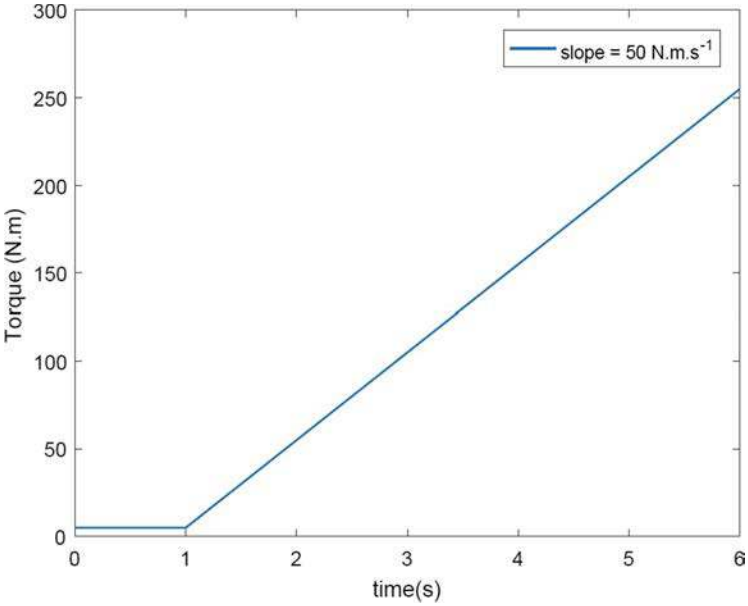

Fig. 7. Torque law as a function of time

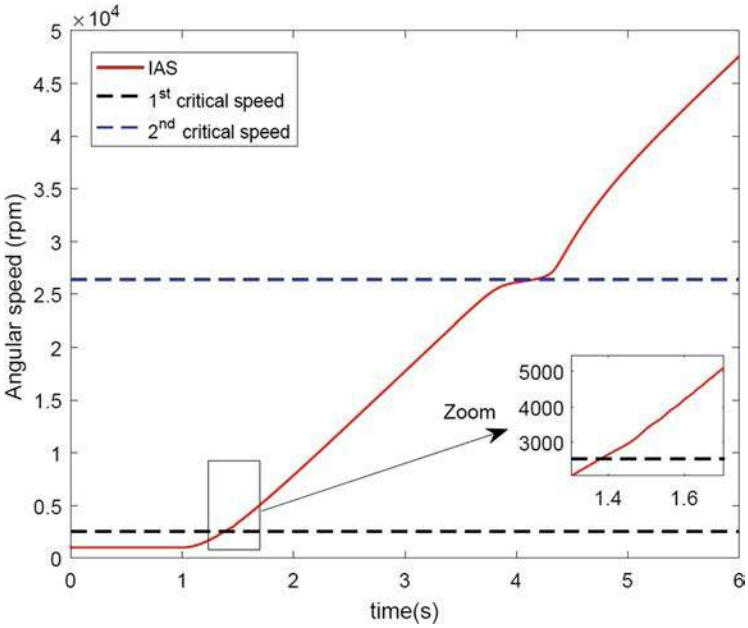

Fig. 8. Instantanious angular speed as a response for the applied torque

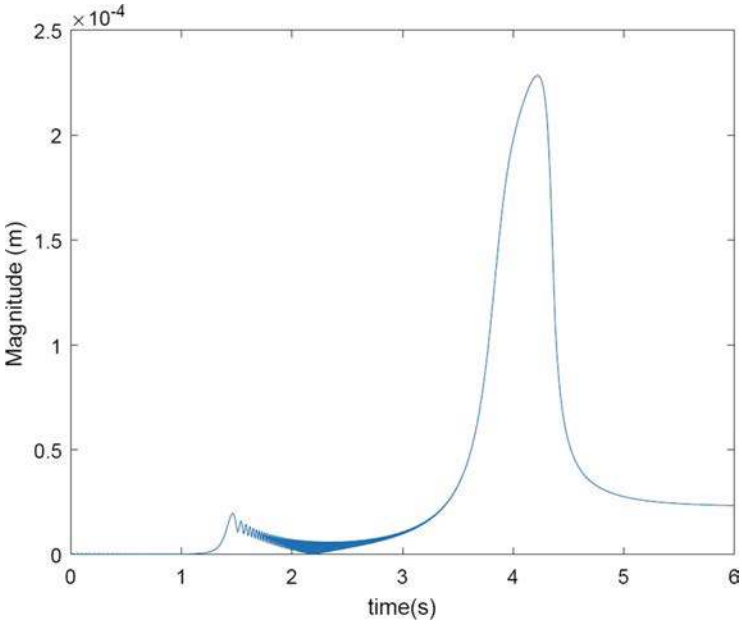

Fig. 9. Lateral displacement when going through two critical speeds

stalls temporarily and then, due to the damping of the system, succeeds on going through this critical speed.

Since the rotor spends longer time around the second critical speed, the amplification of the lateral amplitude is much more important than the amplification of the amplitude when crossing the first critical speed (Fig. 9).

4 Conclusion

The new mathematical model for the dynamic behavior of the rotating machines at non-stationary regime shows coupling between the lateral and torsional degrees of freedom. It also shows strong non-linearities. The results of the simulations show that the model help to better understand the behavior of the rotating machinary. It shows the interaction between the rotational behavior and the lateral one especially in the vicinity of the critical speed. This interaction is usually neglected when considering a given law for the instantanious angular speed. The second step of the presented work will be the establishing of new techniques based on the IAS (Instantaneous Angular Speed) for characterizing the machine behavior and identifing the model parameters at non-stationary working conditions.

Acknowledgments. This work has been done in the context of the RedHV+ project funded by the French State, île de France region, the Auvergne-Rhône-Alpes region

and the county Council of Haute Savoie. The authors would like to thank the RedHV+ team and associated partners. See http://www.redhv.fr/en/

References

1. Lalanne M, Ferraris G (1998) Rotordynamics prediction in engineering. Wiley, Hoboken
2. Genta G, Delprete C (1995) Acceleration through critical speeds of an anisotropic, non-linear, torsionally stiff rotor with many degrees of freedom. J Sound Vib 180(3):369–386
3. Al-bedoor BO (2000) Transient torsional and lateral vibrations of unbalanced rotors with rotor-to-stator rubbing. J Sound Vib 229(3):627–645
4. Roques S, Legrand M, Cartraud P, Stoisser C, Pierre C (2010) Modeling of a rotor speed transient response with radial rubbing. J Sound Vib 329(5):527–546
5. Li L, Singh R (2015) Analysis of transient amplification for a torsional system passing through resonance. Proc Inst Mech Eng Part C: J Mech Eng Sci 229(13):2341–2354
6. Yamamoto T, Kono K (1970) On vibrations of a rotor with variable rotating speed. Bull JSME 13(60):757–765
7. Hsieh S-C, Chen J-H, Lee A-C (2006) A modified transfer matrix method for the coupling lateral and torsional vibrations of symmetric rotor-bearing systems. J Sound Vib 289(1–2):294–333
8. Srinivasan A, Thurston TW (2012) The limited-torque acceleration through critical speed phenomenon in rotating machinery. In: ASME turbo expo 2012: turbine technical conference and exposition. American Society of Mechanical Engineers, pp 607–613